ELSEVIER

Engineering Analysis with Boundary Elements 30 (2006) 702–708

ENGINEERING ANALYSIS with BOUNDARY ELEMENTS

www.elsevier.com/locate/enganabound

Dual error indicators for the local boundary integral equation method in 2D potential problems

X.F. Guo[a,b], H.B. Chen[a,*]

[a]CAS Key Laboratory of Mechanical Behavior and Design of Materials, Department of Modern Mechanics, University of Science and Technology of China, Hefei, Anhui 230026, PR China

[b]Teaching and Research Section of Mechanics, Dalian Jiaotong University, Dalian, Liaoning 116028, PR China

Received 6 July 2005; accepted 14 February 2006
Available online 12 June 2006

Abstract

Three relative error measurements in the numerical solution of potential problems are firstly investigated in detail, and then an algorithm based on the proposed dual error indicators is developed for the meshless local boundary integral equation (LBIE) method. Numerical experiments show that a combined use of the two error indicators is necessary to adequately measure the error of the LBIE solutions.

Keywords: Local boundary integral equation; Regularization; Dual error indicators; Moving least squares; Taylor series expansion

1. Introduction

Recent years, considerable research in computational mechanics has been devoted to the development of meshless methods [1,2]. Among them, the truly meshfree and boundary type algorithms have attracted much attentions. The works of Fairweather and Karageorghis [3] and Cheng [4] involve the method of fundamental solution, a truly meshfree, and easy-to-use boundary method. The boundary knot method (BKM), developed by Chen and Tanaka [5,6], uses the nonsingular general solution to avoid the fictitious boundary outside the physical domain in the method of fundamental solution. The Hybrid boundary node method, proposed by Zhang et al. [7], combines a modified functional with the moving least squares (MLS) approximation. The boundary particle method proposed by Chen [8] is a truly boundary-only meshfree method for inhomogeneous problems. The local boundary integral equation (LBIE) method has been introduced by Zhu et al. [9] for potential problem, which has the advantages when geometrical and material nonlinearities and nonhomogeneous material properties are analyzed [10–12].

Some works on error estimations for meshless methods have been done referring to the related finite element method (FEM) or boundary element method (BEM) research. Gavete et al. [13,14] used two different procedures to estimate numerical error in element free Galerkin method: one through direct gradient calculation and the other through MLS using Taylor series expansion. The singular and hpyersingular boundary node methods (BNMs) have been employed for the usual and adaptive solutions of three-dimensional potential and elasticity problems by Chati et al. [15]. Duarte and Oden [16] proposed an *h–p* adaptive method using clouds. Furthermore, Liu et al. [17] developed *h*, *p* and *hp* adaptive meshless method for plane crack problem, and so on. However, these researches are focused on meshless methods with background cells for integrals. To our knowledge, there is no report involving the error estimate of the LBIE approach [9–12] — a true meshless method. It may be due to that LBIE approach is a particular meshless method without any elements or cells for approximation and integration making its error estimation difficult.

*Corresponding author. Tel.: +86 551 3603724; fax: +86 551 3606459
E-mail address: hbchen@ustc.edu.cn (H.B. Chen).

0955-7997/$ - see front matter © 2006 Elsevier Ltd. All rights reserved.
doi:10.1016/j.enganabound.2006.02.009

Error estimation and adaptive mesh or node refinement for a numerical analysis are generally based on the following three ideas: (1) from the problem governing equation, as the regular boundary integral equation and the regular hypersingular boundary integral equation have been employed together in the BNM [15]; (2) from the interpolated/approximated trial function, as it is easy to implement *p*-refinement in *h–p* clouds [16]; (3) from some a-posteriori techniques in FEM or BEM, as Jorge et al. [18] used the smoothed boundary tangential potential derivatives in 2D BEM potential problem and Gavete et al. [14] used the Taylor series expansion in element free Galerkin method. When the errors of some elements or nodes are too big and not to meet the error criteria, it is necessary to use some schemes to refine the mesh or nodal distribution in order to reduce these errors. Refinement schemes for the traditional boundary element method are basically classified into the *h*-refinement where the total number of elements or nodes is increased, the *p*-refinement where the order of interpolation function is increased uniformly or selectively, the *r*-refinement where the mesh points are relocated within fixed topology and their combinations schemes [18–23]. In the adaptivity meshless methods, *h*-refinement only needs to add some new nodes in the high error region and is easy to accomplish without the requirement of the nodal relation information [13–15]. On the other hand, because all freedoms are focused on the nodes and conformability is not required in the meshless methods, *p*-refinement is also easy to implement and often has more efficient convergence than *h*-refinement [16,17]. However, due to the complexity and the relatively short time in the research of adaptivity meshless methods, many problems remain unresolved.

In this paper, after three error estimation schemes are compared in detail, a dual error indicator for LBIE method is proposed. Numerical examples show the feasibility to employ the two error indicators together in accessing the quality when adding new nodes in nodal distribution refinement.

2. The regularized local boundary integral equation

The Cauchy singularity exists in LBIE method when the node locates on the boundary. Concerning the elimination algorithm used in the conventional BEM [24,25], a regularized formulation is applied for the present LBIE, called the regularized LBIE (RLBIE). The RLBIE holds over $\partial\Omega_s$, the boundary of the sub-domain Ω_s:

$$0 = \int_{\partial\Omega_s} u^{**}(\vec{x},\vec{y})\frac{\partial u(\vec{x})}{\partial n}\mathrm{d}\Gamma_x - \int_{\partial\Omega_s}\frac{\partial u^{**}(\vec{x},\vec{y})}{\partial n_x}(u(\vec{x}) - u(\vec{y}))\,\mathrm{d}\Gamma_x, \tag{1}$$

where $\vec{y}$ is the source point, $\vec{x}$ is the integration point, and

$$u^{**}(\vec{x},\vec{y}) = \frac{1}{2\pi}\ln\frac{r_0}{r(\vec{x},\vec{y})}$$

is the modified test function for Laplacian equation problem [26]. The sub-domain Ω_s is assumed to be intersection of the analyzed domain Ω with the circular domain Ω_s' of the radius r_Ω and centered at $\vec{y}$.

The LBIE formulation does not show singularity when the node is located inside the analyzed domain, and thus it is not necessary to regularize the equation in this case. Therefore, the regularized Equation (1) is used only for the boundary nodes, i.e.

$$u(\vec{y}) = -\int_{L_s} u(\vec{x})\frac{\partial u^{**}(\vec{x},\vec{y})}{\partial n_x}\mathrm{d}\Gamma \quad \text{for interior node,} \tag{2a}$$

$$0 = \int_{\Gamma_s} u^{**}(\vec{x},\vec{y})\frac{\partial u(\vec{x})}{\partial n}\mathrm{d}\Gamma_x - \int_{\partial\Omega_s}(u(\vec{x}) - u(\vec{y}))\frac{\partial u^{**}(\vec{x},\vec{y})}{\partial n_x}\mathrm{d}\Gamma \quad \text{for boundary node.} \tag{2b}$$

Denoting by L_s the circular part of the boundary $\partial\Omega_s$, i.e. $L_s = \partial\Omega_s \cap \partial\Omega_s'$, one can see that $u^{**}(\vec{x},\vec{y})$ vanishes on L_s. Furthermore, it is assumed that for an interior node $\vec{y}$ the associated sub-domain $\Omega_s = \Omega_s'$, hence $\Gamma_s = \partial\Omega_s - L_s = \varnothing$ or $\partial\Omega_s = L_s = \partial\Omega_s'$.

In the current work, the MLS approximation is used to represent the trial function with the fictitious values of the unknown variable at the randomly located nodes

$$u^h(\vec{x}) = \boldsymbol{\Phi}^{\mathrm{T}}_{1\times N}\hat{\boldsymbol{u}}_{N\times 1} = \sum_{I=1}^{N}\phi_I(\vec{x})\hat{u}_I. \tag{3}$$

Discretizations of the LBIE are as follows, for interior nodes:

$$K_{Ij}' = -\int_{L_s}\phi_j(\vec{x})\frac{\partial u^{**}}{\partial n_x}\mathrm{d}\Gamma_x, \tag{4a}$$

$$f_I' = 0. \tag{4b}$$

for boundary nodes: (A) for node I with $u(\vec{y})$ unknown,

$$K_{Ij}' = \int_{\Gamma_{su}} u^{**}\frac{\partial\phi_j(\vec{x})}{\partial n}\mathrm{d}\Gamma_x - \int_{\Gamma_{su}}\left(-\phi_j(\vec{y})\right)\frac{\partial u^{**}}{\partial n_x}\mathrm{d}\Gamma_x - \int_{\Gamma_{sq}}\left(\phi_j(\vec{x}) - \phi_j(\vec{y})\right)\frac{\partial u^{**}}{\partial n_x}\mathrm{d}\Gamma_x - \int_{L_s}\left(\phi_j(\vec{x}) - \phi_j(\vec{y})\right)\frac{\partial u^{**}}{\partial n_x}\mathrm{d}\Gamma_x, \tag{5a}$$

$$f_I' = \int_{\Gamma_{sq}} u^{**}\bar{q}\,\mathrm{d}\Gamma_x - \int_{\Gamma_{su}}\bar{u}\frac{\partial u^{**}}{\partial n_x}\mathrm{d}\Gamma_x. \tag{5b}$$

(B) for node I with $u(\vec{y})$ prescribed,

$$K_{Ij}' = \int_{\Gamma_{su}} u^{**}\frac{\partial\phi_j(\vec{x})}{\partial n}\mathrm{d}\Gamma_x - \int_{\Gamma_{sq}}\phi_j(\vec{x})\frac{\partial u^{**}}{\partial n_x}\mathrm{d}\Gamma_x - \int_{L_s}\phi_j(\vec{x})\frac{\partial u^{**}}{\partial n_x}\mathrm{d}\Gamma_x, \tag{6a}$$

$$f'_I = \int_{\Gamma_{sq}} u^{**}\bar{q}\,\mathrm{d}\Gamma_x - \int_{\Gamma_{su}} (\bar{u}-\bar{u}(\vec{y}))\frac{\partial u^{**}}{\partial n_x}\mathrm{d}\Gamma_x - \int_{\Gamma_{sq}} (-\bar{u}(\vec{y}))\frac{\partial u^{**}}{\partial n_x}\mathrm{d}\Gamma_x - \int_{L_s} (-\bar{u}(\vec{y}))\frac{\partial u^{**}}{\partial n_x}\mathrm{d}\Gamma_x. \quad (6b)$$

At last, one can get the following linear equation system:

$$\mathbf{K}\hat{\boldsymbol{u}} = \boldsymbol{f}. \quad (7)$$

Where

$$\begin{cases} K_{Ij} = -K'_{Ij} + \phi_j(\vec{\boldsymbol{x}}_I) \\ f_I = f'_I \end{cases} \text{ for interior node I,}$$

$$\begin{cases} K_{Ij} = -K'_{Ij} \\ f_I = f'_I \end{cases} \text{ for boundary node I.}$$

3. Moving Least Squares approximation using Taylor series expansion

In this paper, when adding a new node in the procedure of nodal distribution refinement, the new node is put at the middle of two original nodes. Consider three set solutions: the first calculated by normal MLS through the fictitious potentials of the original nodes; the second obtained by MLS using Taylor series expansion, but only for the newly added nodes; and the third calculated by MLS through the fictitious potentials of the original and newly added nodes together, after a reanalysis has been performed.

In order to calculate the second solution, a Taylor expansion around point $P(x_i,y_i)$ can be expressed in the form

$$u = u_i + h\frac{\partial u_i}{\partial x} + k\frac{\partial u_i}{\partial y} + o(\rho^2), \quad (8)$$

where $u = u(x,y)$, $u_i = u(x_i,y_i)$, $h = x - x_i$, $k = y - y_i$, $\rho = \sqrt{h^2+k^2}$.

Consider norm B

$$B = \sum_{I=1}^{N_i} w_I(\vec{\boldsymbol{x}} - \vec{\boldsymbol{x}}_I)\left[u_i + h_I\frac{\partial u_i}{\partial x} + k_I\frac{\partial u_i}{\partial y} - u_I\right]^2, \quad (9)$$

where the N_i points are those nodes close to the evaluation point $P(x_i,y_i)$, and $h_I = x_I - x_i$, $k_I = y_I - y_i$. In this paper, $N_i = N/2$ when N is an even number and $N_i = (N-1)/2$ when N is an odd number, where N is the total node number of a discretization.

The solution may be obtained by minimizing norm B

$$\frac{\partial B}{\partial\{Du\}} = 0, \quad (10)$$

where

$$\{Du\}^{\mathrm{T}} = \left[u_i, \frac{\partial u_i}{\partial x}, \frac{\partial u_i}{\partial y}\right]. \quad (11)$$

The expansion of Eq. (10) is

$$\begin{bmatrix} \Sigma w_I & \Sigma w_I h_I & \Sigma w_I k_I \\ \Sigma w_I h_I & \Sigma w_I h_I^2 & \Sigma w_I h_I k_I \\ \Sigma w_I k_I & \Sigma w_I h_I k_I & \Sigma w_I k_I^2 \end{bmatrix} \begin{Bmatrix} u_i \\ \frac{\partial u_i}{\partial x} \\ \frac{\partial u_i}{\partial y} \end{Bmatrix} = \begin{Bmatrix} \Sigma u_I w_I \\ \Sigma u_I w_I h_I \\ \Sigma u_I w_I k_I \end{Bmatrix}, \quad (12)$$

where $\sum$ is the abbreviation of $\sum_{I=1}^{N_i}$.

4. Numerical examples

The relative errors in the numerical examples are defined as

$$\varepsilon_i = \frac{\left|u_i^{(numerical)} - u_i^{(exact)}\right|}{\left(\sum_{j=1}^{N}\left|u_j^{(exact)}\right|\right)/N} \times 100\% \quad (13)$$

where i denotes the evaluation point and N is the total node number of a discretization. The three sets of potential solution are: "Original" denotes the potential calculated by MLS through the fictitious values at original nodes; "Taylor" denotes the potential obtained by MLS using Taylor series expansion, for the newly added nodes; "Refresh" denotes the potential calculated by MLS through the fictitious values at the original and newly added nodes, after a reanalysis of the local boundary integral equations has been performed.

Example 1. Fig. 1 defines a circular section under torsion. The analytical solution of this problem is

$$u = a\left(r + \frac{b^2}{r}\right)\sin\theta,$$

where u is the warping function. In this example, $a = 2, b = 1$ and a mixed boundary conditions are prescribed. The potential along arc ABC is $4\sin\theta$ and the flux along arc CDA is y. The number of nodes in the initial discretization is 15, including 14 boundary nodes and only one internal node. The nodal arrangements with seven and

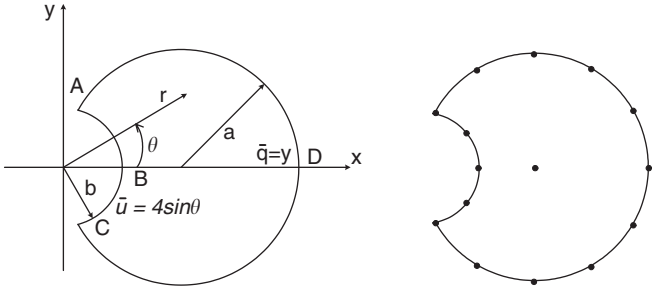

Fig. 1. A circular section under torsion and its initial discretization with 15 nodes.

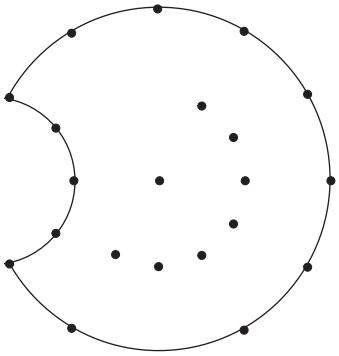

Fig. 2. Nodal arrangement with seven additional nodes.

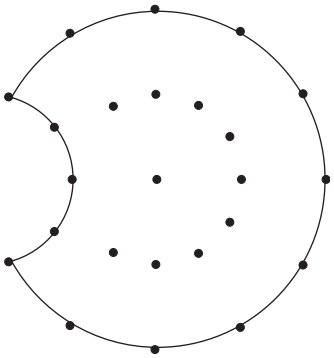

Fig. 3. Nodal arrangement with nine additional nodes.

nine additional (newly added) nodes are shown in Figs. 2 and 3, respectively.

Fig. 2 shows the nodal arrangement with seven additional nodes, dense at the down half and right of the circular section but sparse at the up-left of the section. In Fig. 4, the nodes from No. 16 to 22 correspond to the additional middle points, and the "Taylor" results at No. 1–15 are the same as the "Original" ones. There are two additional points whose "Taylor" errors are much lower than their "Original" ones. The "Taylor" errors of other middle points are similar to their "Original" ones and they are relatively at a low level. When LBIEs are solved again for the original and newly added nodes together, the "Refresh" errors are globally not reduced compared with the "Original" ones. This shows that the nodal arrangement with seven additional points in this distribution is not a good one.

Fig. 3 shows the nodal arrangement with 9 additional middle points distributed uniformly. In Fig. 5, the nodes from No. 16 to 24 correspond to the newly added middle points. There are four additional points whose "Taylor" errors are much lower than their "Original" ones. The "Taylor" errors of other middle points are similar to their "Original" ones and they are at a low level. When the problem is solved again for the new nodal distribution, the "Refresh" errors for all the nodes reduce obviously compared with the "Original" ones. It shows that the nodal arrangement is well-distributed.

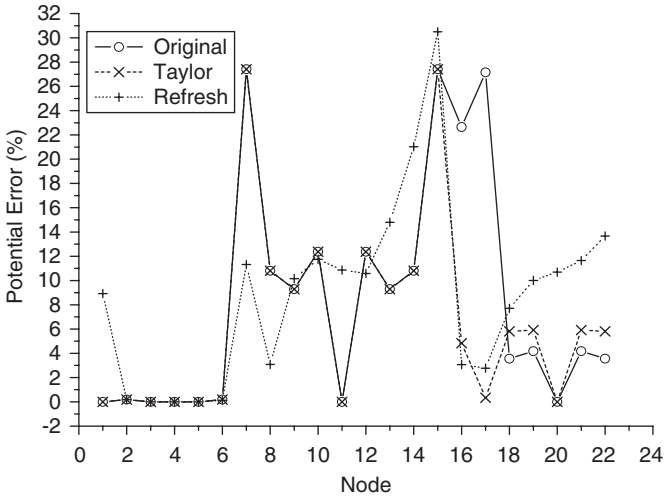

Fig. 4. Error comparison with seven additional nodes.

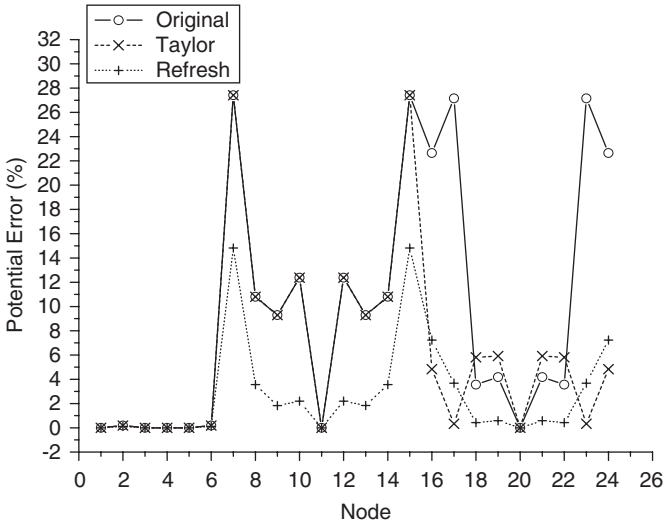

Fig. 5. Error comparison with nine additional nodes.

Example 2. Consider a plane potential flow around a cylinder of radius a in an infinite domain, shown in Fig. 6. Because of symmetry, only one quarter of the domain needs to be analyzed. Fig. 7 shows the model with boundary conditions and the initial nodal arrangement with 19 nodes (16 boundary nodes and three internal nodes). The exact solution can be expressed as

$$u = V_\infty y\left[1 - \frac{a^2}{(x-L)^2 + y^2}\right] = y\left[1 - \frac{1}{(x-4)^2 + y^2}\right],$$

where u represents the flow function, V_∞ is the horizontal flow velocity at infinite distance, $(L, 0)$ is the location of the cylinder. Figs. 8 and 9 are the nodal arrangements with 15 and 8 additional points, respectively.

In Fig. 10, the nodes from No. 20 to 34 correspond to the additional middle points. Globally, the "Taylor" errors of the additional nodes decrease obviously compared with their "Original" ones. When solving again, the "Refresh"

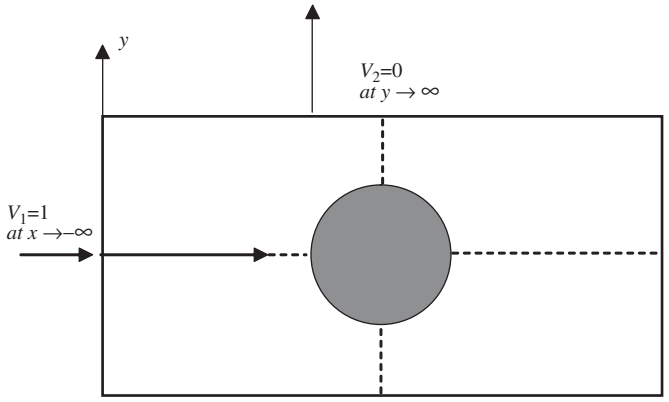

Fig. 6. Flow around a cylinder in an infinite field.

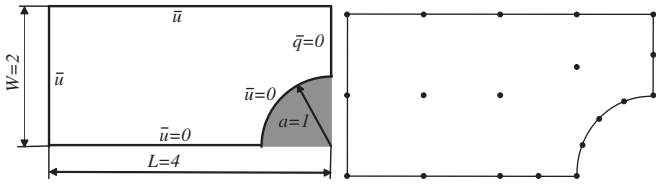

Fig. 7. The model with boundary conditions and its initial discretization with 19 nodes.

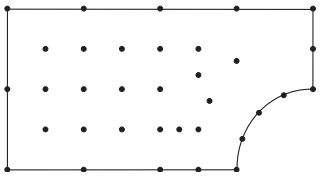

Fig. 8. Nodal arrangement with 15 additional nodes.

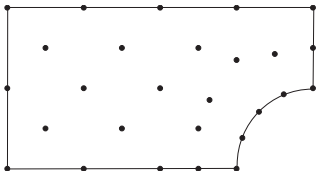

Fig. 9. Nodal arrangement with eight additional nodes.

errors of some additional nodes decrease but others increase, particularly one of them increases obviously. It illustrates that the nodal arrangement is not desirable.

In Fig. 11, the nodes from No. 20 to 27 correspond to the additional middle points. For the additional new nodes, both "Taylor" and "Refresh" errors are globally decreased compared with their "Original" ones. Furthermore, the "Refresh" maximum error for the original nodes also reduces obviously. It shows that the nodal arrangement is well-distributed.

Example 3. This example analyzes the potential problem in an L-shaped domain with mixed boundary conditions, as shown in Fig. 12. The analytical solution is

$$u(r,\theta) = r^{2/3}\sin(2\theta/3),$$

where r and θ are the polar coordinates. There is a singular point at the reentrant corner o for potential derivatives. The

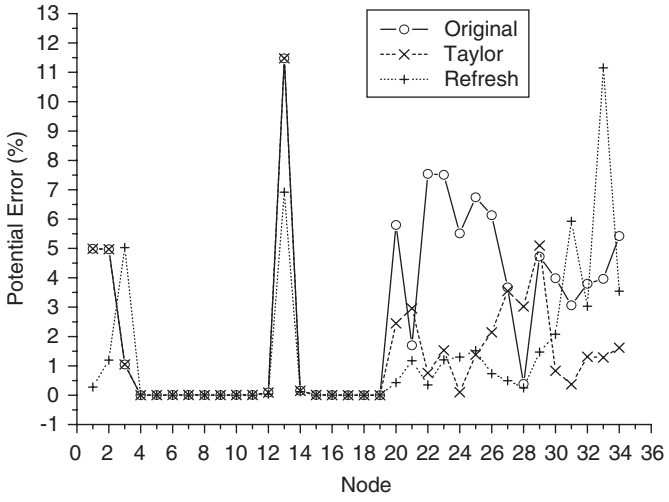

Fig. 10. Error comparison with 15 additional nodes.

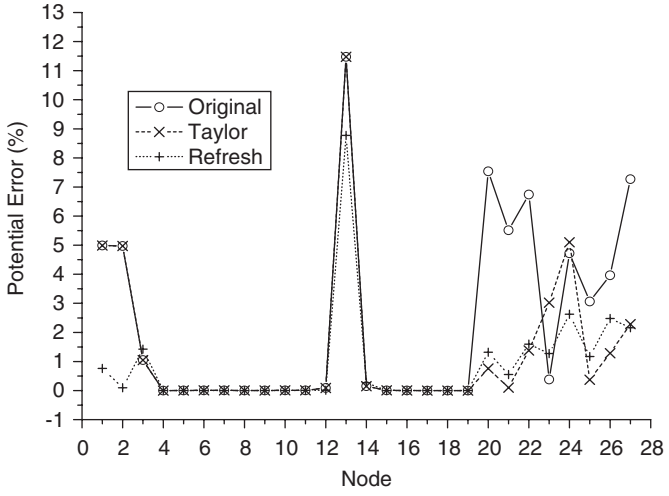

Fig. 11. Error comparison with eight additional nodes.

initial nodal arrangement was discretized with 21 nodes including 16 boundary nodes and five internal nodes, as also shown in Fig. 12. Two nodal arrangements with additional 10 and 18 points can be seen in Figs. 13 and 14, respectively.

In Fig. 15, the nodes from No. 22 to 31 correspond to the additional middle points. The "Taylor" errors of almost all the new points fall down in different degrees compared with their "Original" ones, while globally "Refresh" errors increase obviously at both the original and the additional nodes. It shows that the nodal arrangement in this distribution is not good.

In Fig. 16, the nodes from No. 22 to 39 correspond to the new additional points and similar phenomenon can be observed as in Examples 1 and 2 for the well-distributed cases.

5. Dual error indicators for the local boundary integral equation method

The above three examples illuminate the following phenomenon: (1) for the newly added nodes, the "Taylor"

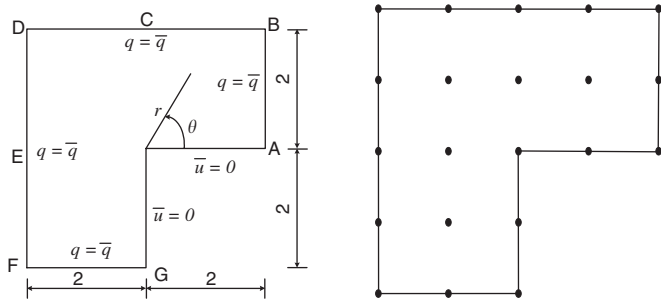

Fig. 12. An L-shaped domain with reentrant corner singularity and its initial discretization with 21 nodes.

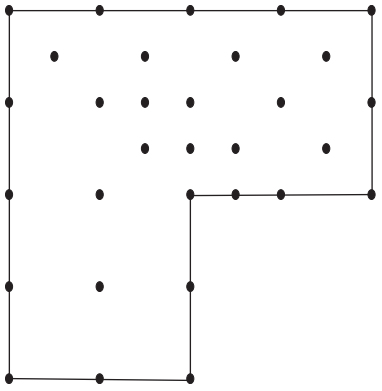

Fig. 13. Nodal arrangement with 10 additional nodes.

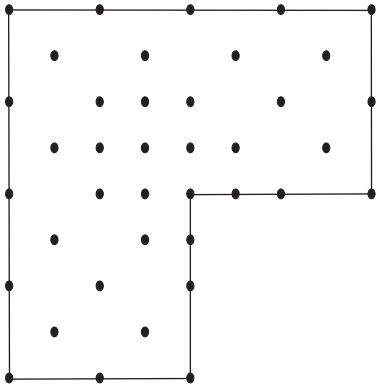

Fig. 14. Nodal arrangement with 18 additional nodes.

errors are always lower than their "Original" ones; (2) when the newly added nodes and the original ones are combined together and the LBIE formulation is solved again, the magnitude of the solution error, i.e. the "Refresh" error, depends on the quality of the new nodal distribution. Compared with the "Original" errors, when the new nodal distribution is good, the "Refresh" errors reduce obviously; on the other hand, when the distribution is not desirable, the "Refresh" errors are generally unstable and their maximum error may surpass the "Original" one; and (3) in the well-distributed arrangements, the "Refresh" errors are similar to the "Taylor" ones at the newly added nodes.

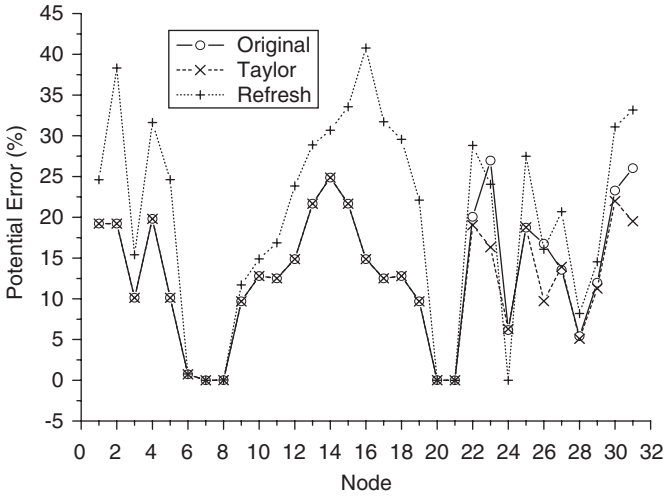

Fig. 15. Error comparison with 10 additional nodes.

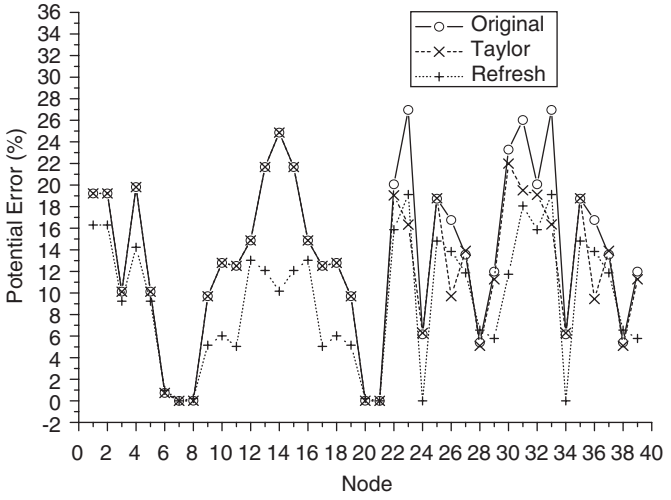

Fig. 16. Error comparison with 18 additional nodes.

Generalizing the above conclusions, application of the dual error indicators for the meshless LBIE method is preliminarily proposed in this paper:

(1) The quality of the initial nodal arrangement should be tested firstly. Add new nodes in the sparse area and then judge whether to redistribute the nodes.

(2) When an adaptive nodal distribution refinement is implemented, new additional nodes are advised to locate at the middle points on the lines between two neighbor nodes for internal region and also at the middle points of the boundary contours between two neighbor boundary nodes. The way of so adding new nodes, not only is easy to implement, but also can judge whether to add a new node or not.

(3) To implement the dual error indicators algorithm to a general problem with no exact solution, three sets of solution should be defined as: the first solutions including new additional points calculated by MLS through the original nodal fictitious values; and then the second

solutions for new additional points calculated by MLS using Taylor series expansion; at last, the third solutions calculated by MLS through the new nodal fictitious values after a reanalysis of the LBIEs is performed for the original and newly added nodes together. One error indicator is defined by the first two solutions, but because it is uncertain whether the new nodal arrangement would be well-distributed, another error indicator is defined by the first and the third solutions to judge the quality of the former one. When these two error indicators are consistent with each other, the nodal arrangement with new additional points is well-distributed; otherwise, modulate the location and number of the new additional nodes.

6. Conclusion and discussions

As the local boundary integral equation method has some special characteristics, i.e. the interpolation approximation of the trial function with the values (or the fictitious values) of the unknown variable at the randomly located nodes and the local effects of local boundary integral equations, it is not an easy task to implement the error estimation and adaptive refinement for this meshless method. After analyzing the three sets of relative errors in detail, a dual error indicators algorithm is proposed in this paper. So far as we learn from the literature, this work is the first research on the LBIE error estimation, and it is novel in the field of error estimation and adaptive mesh refinement research. The aim to solve the LBIEs again in the new nodal distribution is to check the effect of the new additional points on the next-solving results and is to make sure that the new nodal arrangement would be well-distributed.

It should be stressed that the research and discussions on the error indicator and adaptive refinement for the meshless LBIE method in this paper are preliminary, and many problems should be further investigated. For instance, the present numerical experiments can only illustrate the necessity of using two error indicators at the same time, how to define the two residual properly and to develop an effective refinement procedure for the nodal distribution require more investigations. Furthermore, the examples in this paper belong to *h*-refinement, how to apply the present idea to *p*- and *r*-refinements requires further research. However, the initial work here holds significant possibilities for the future of adaptive numerical analysis for the LBIE method and the other meshfree algorithms.

References

[1] Belytschko T, Krongauz Y, Organ D, Fleming M, Krysl P. Meshless methods: an overview and recent developments. Comput Meth Appl Mech Eng 1996;139:3–47.

[2] Fries TP, Hermann GM. Classication and overview of mesh- free methods. Germany: Institute of Scientic Computing, Technical University Braunschweig Brunswick, Germany; 2003.

[3] Fairweather G, Karageorghis A. The method of fundamental solutions for elliptic boundary value problems. Adv Comput Math 1998;9:69–95.

[4] Cheng AHD. Particular solutions of Laplacian, Helmholtz-type, and polyharmonic operators involving higher order radial basis functions. Eng Anal Bound Elem 2000;24:531–8.

[5] Chen W, Tanaka M. A meshless exponential convergence, integration-free, and boundary-only RBF technique. Computers Math Appl 2002;43:379–91.

[6] Chen W. Symmetric boundary knot method. Eng Anal Bound Elem 2002;26(6):489–94.

[7] Zhang JM, Yao ZH, Li H. A hybrid boundary node method. Int J Numer Methods Eng 2002;53:751–63.

[8] Chen W. Meshfree boundary particle method applied to Helmholtz problems. Eng Anal Bound Elem 2002;26(7):577–81.

[9] Zhu T, Zhang JD, Atluri SN. A local boundary integral equation (LBIE) method in computational mechanics and a meshless discretization approach. Comput Mech 1998;21(3):223–35.

[10] Sladek J, Sladek V, Atluri SN. Local boundary integral equation (LBIE) method for solving problems of elasticity with nonhomogeneous material properties. Comput Mech 2000;24(6):456–62.

[11] Sladek J, Sladek V, Atluri SN. Application of the local boundary integral equation method to boundary-value problems. Int Appl Mech 2002;38(9):1025–47.

[12] Sellountos EJ, Polyzos D. A meshless local boundary integral equqtion method for solving transient elastodynamic problems. Comput Mech 2005;35(4):265–76.

[13] Gavete L, Falcón S, Ruiz A. An error indicator for the element free Galerkin method. Eur J Mech A/Solids 2001;20(2):327–41.

[14] Gavete L, Cuesta JL, Ruiz A. A numerical comparison of two different approximations of the error in a meshless method. Eur J Mech A/Solids 2002;21:1037–54.

[15] Chati MK, Paulino GH, Mukherjee S. The meshless standard and hypersingular boundary node methods-applications to error estimation and adaptivity in three dimensional problems. Int J Numer Methods Eng 2001;50(9):2233–69.

[16] Duarte CA, Oden JT. An *h–p* adaptive method using clouds. Comput Meth Appl Mech Eng 1996;139:237–62.

[17] Liu X, Zhu D, Lu M, Zhang X. *h*, *p*, *hp* Adaptive meshless method for plane crack problem. Acta Mech Sinica 2000;32(3):308–18.

[18] Jorge AB, Ribeiro GO, Fisher TS. New approaches for error estimation and adaptivity for 2D potential boundary element methods. Int J Numer Meth Eng 2003;56:117–44.

[19] Liang MT, Chen JT, Yang SS. Error estimation for boundary element method. Eng Anal Bound Elem 1999;23:257–65.

[20] Kita E, Kamiya N. Error estimation and adaptive mesh refinement in boundary element method: an overview. Eng Anal Bound Elem 2001;25:479–95.

[21] Rodríguez JJ, Power H. *h*-Adaptive mesh refinement strategy for the boundary element method based on local error analysis. Eng Anal Bound Elem 2001;25:565–79.

[22] Chen JT, Chen KH, Chen CT. Adaptive boundary element method of time-harmonic exterior acoustics in two dimensions. Comput Methods Appl Mech Eng 2002;191:3331–45.

[23] Chen HB, Yu DH, Schnack E. A simple a-posteriori error estimation for adaptive BEM in elasticity. Comput Mech 2003;30:343–54.

[24] Chen HB, Lu P, Huang MG, Williams FW. An effective method for finding values on and near boundaries in elastic BEM. Comput Struct 1998;69:421–31.

[25] Chen HB, Lu P, Schnack E. Regularized algorithms for the calculation of values on and near boundaries in the elastic BEM. Eng Anal Bound Elem 2001;25:851–76.

[26] Guo XF. The study on error indicator and mesh refinement for BEM/LBIEM. Master thesis, University of Science and Technology of China, 2005.